ADVANCED FUNCTIONAL MATERIALS
www.afm-journal.de

Materials Views
www.MaterialsViews.com

Micropatterning Alginate Substrates for In Vitro Cardiovascular Muscle on a Chip

*Ashutosh Agarwal, Yohan Farouz, Alexander Peyton Nesmith, Leila F. Deravi, Megan Laura McCain, and Kevin Kit Parker**

Soft hydrogels such as alginate are ideal substrates for building muscle in vitro because they have structural and mechanical properties close to the in vivo extracellular matrix (ECM) network. However, hydrogels are generally not amenable to protein adhesion and patterning. Moreover, muscle structures and their underlying ECM are highly anisotropic, and it is imperative that in vitro models recapitulate the structural anisotropy in reconstructed tissues for in vivo relevance due to the tight coupling between sturcture and function in these systems. Two techniques to create chemical and structural heterogeneities within soft alginate substrates are presented and employed to engineer anisotropic muscle monolayers: i) microcontact printing lines of extracellular matrix proteins on flat alginate substrates to guide cellular processes with chemical cues and ii) micromolding of alginate surface into grooves and ridges to guide cellular processes with topographical cues. Neonatal rat ventricular myocytes as well as human umbilical artery vascular smooth muscle cells successfully attach to both these micropatterned substrates leading to subsequent formation of anisotropic striated and smooth muscle tissues. Muscular thin film cantilevers cut from these constructs are then employed for functional characterization of engineered muscular tissues. Thus, micropatterned alginate is an ideal substrate for in vitro models of muscle tissue because it facilitates recapitulation of the anisotropic architecture of muscle, mimics the mechanical properties of the ECM microenvironment, and is amenable to evaluation of functional contractile properties.

1. Introduction

Cardiac pumping arises from the contraction of elongated cardiac myocytes arranged in layered anisotropic bands around the ventricular cavities. Similarly, vascular tone in arteries carrying blood from the heart arises from the highly elongated and anisotropic architecture of smooth muscle tissues that wrap circumferentially around the lumen. Hence, recreating anisotropic muscle structure is a critical requisite for construction of functional in vitro models of contractile muscle. In the past, efforts have been made to control engineered cardiovascular muscle architecture by changing the topographical cues from the micro[1,2] to nanoscale[3] or by the use of oriented nanofibers.[4,5] Previously, it has been reported that microcontact printing can be employed for creating confluent monolayers of aligned cardiac myocytes[6–8] and vascular smooth muscle[9,10] which show mature, functional cytoskeletal assemblies. Muscular thin films (MTFs) have been constructed by engineering muscular tissues on top of thin elastomeric cantilevers and it has been shown that tissues with controlled architecture exhibit stronger contraction.[6–10]

In addition to tissue architecture, the mechanical properties of the cellular microenvironment plays a key role in muscle functionality[11,12] and differentiation.[13,14] To better mimic the stiffness of cardiac tissue, synthetic and natural biodegradable materials such as polycaprolactone, poly(glycerol sebacate), gelatin and alginate have been utilized as substrates.[15,16] Alginate is a naturally occurring block co-polymer and has been extensively studied for in vivo biomedical applications due to its low immunogenicity as well as tunability of stiffness, ease of gelation, sustained drug release, and attachment of cell adhesive peptides/proteins.[17,18] In cardiovascular applications, alginate-based scaffolds have been used either to improve cardiac function after myocardial infarction,[19,20] to deliver stem cells into the infarcted area,[21] to promote the adhesion of cardiac myocytes,[22] or to induce neovascularization of the infarcted area.[23] In general, studies that have employed alginate substrates for tissue engineering applications have either engineered the substrate topography[24] or the substrate stiffness,[25] but not simultaneously.

In this study, we sought to design a biomaterial with embedded cues to direct the assembly of anisotropic cardiovascular muscle tissue that also recapitulates the stiffness of muscle tissue in vivo and is amenable to functional measurements. We identified alignate as a substrate because its reversible crosslinking by diffusion of calcium allows for the control of shape (surface topography), thickness, as well as stiffness of the material. Alginate films were attached to aminosilane modified glass coverslips. To facilitate attachement of fibronectin, a native

A. Agarwal, Y. Farouz, A. P. Nesmith, L. F. Deravi, M. L. McCain, K. K. Parker
Disease Biophysics Group
Wyss Institute for Biologically Inspired Engineering
School of Engineering and Applied Sciences
Harvard University
29 Oxford St, Pierce Hall 321, Cambridge, MA, USA
E-mail: kkparker@seas.harvard.edu

DOI: 10.1002/adfm.201203319

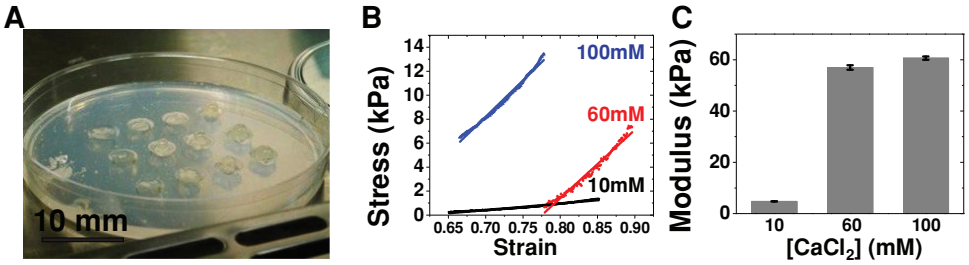

Figure 1. Mechanical characterization of 5% w/v of alginate. A) Example photograph of 12 test samples punched out for mechanical testing. B) Stress-strain curve collected for alginate substrates ionically crosslinked with 10, 60, and 100 mM $CaCl_2$. The straight line fits reveal a strong linear correlation implying elastic behavior. C) Young's moduli for 10, 60, and 100 mM $CaCl_2$ conditions calculated from the corresponding slope of the linear fits were determined to be 4.77 ± 0.08 kPa, 56.98 ± 0.86 kPa and 60.60 ± 0.64 kPa respectively (Mean ± SEM, N = 3 samples).

ECM protein, streptavidin was covalently coupled to alginate and biotin-streptavidin interactions were used to control the surface density and spatial distribution of fibronectin. Anisotropic cardiac and vascular smooth muscle tissue were engineered on these micropatterned soft hydrogel surfaces, which were then cut into cantilevers and used to measure muscle contractility. These efforts fit well and build upon the "muscle-on-a-chip" technologies that have been previously reported for engineered muscle tissues in vitro and quantifying tissue contractility.[6–10]

2. Results

2.1. Modulating Stiffness of Alginate Scaffolds

The mechanical properties of alginate can be controlled by a number of independent methods such as molecular weight and distribution of its constituents and type and concentration of ionic and covalent cross-linking agents.[25] Divalent calcium is widely used as a reversible ionic cross-linker and thus we asked if alginate stiffness could be tailored with varying calcium ion concentration. **Figure 1** depicts the results from mechanical testing of cylindrical alginate gel disks (height: 1 mm, diameter: 8 mm; test samples photograph in Figure 1A) crosslinked by 10, 60, and 100 mM $CaCl_2$. For all gels, R^2 values for the linear fits were greater than 0.95 (Figure 1B). Hence, Young's modulus in compression was assumed to be equal to the slope of the linear fit within those deformation ranges. The non zero intercepts on both X and Y axes are a result of the deformation being recorded in the instrument before the test sample comes in contact with the top and bottom compression platens. The corresponding compressive moduli data (plotted in Figure 1C) suggest that calcium ion concentration within the alginate gels may be approaching saturation at concentrations close to 60 mM. In an attempt to match the stiffness of the native myocardium (reported values range from 10 to 70 kPa),[26–28] we performed all the following experiments using a concentration of 60 mM of $CaCl_2$ and 5% w/v of alginate. A gel with Young's modulus of 57 kPa falls within the range of stiffness usually obtained with polyacrylamide gels[29] and is two orders of magnitude softer than polydimethylsiloxane (PDMS)[30]– two materials commonly employed in in vitro tissue models.

2.2. Microcontact Printing of Fibronectin on Alginate thin Films

Alginate hydrogels are generally protein non-fouling and lack mammalian cell adhesivity. Hence, we sought to develop a novel and efficient technique to pattern fibronectin onto alginate thin films through specific streptavidin-biotin interactions. As illustrated in **Figure 2**, a crosslinked alginate film (Figure 2Ai–iii) is first functionalized with streptavidin (Figure 2Aiv). Next, microcontact printing technique is used to transfer biotinylated fibronectin on top of the alginate thin film via a PDMS stamp (Figure 2Av–vi). Microcontact printed biotinylated fibronectin matched accurately the feature geometry of the stamp, as revealed by a fibronectin immunostain in Figure 2Bi and the corresponding line fluorescence scan in Figure 2Bii. Thus, we successfully functionalized the surface of alginate to facilitate micropatterning of fibronectin.

2.3. Micromolding of Alginate thin Films

Capillary force lithography has recently been developed for micromolding of gels and exerting microscale control over their topography.[31,32] We adapted that technique by taking advantage of calcium diffusion through a molded agar stamp to fabricate ridges and grooves within the alginate surface. To fabricate micromolded films of alginate, a 40 µL drop of 5% alginate was pressed between an aminosilane-functionalized 18mm diameter glass coverslip and a patterned agar stamp (Figure 2Ci–v). Release of the gelling agent (calcium ions) and subsequent gelling was complete within 60 seconds, leaving behind a negative replica of the features on the agar stamp. After removal of the stamp, the coverslips were stored in a solution of 1% $CaCl_2$, in order to maintain equilibrium of calcium concentration. The features of the molded alginate were found to be consistent with the equivalent pattern using micropatterning (Figure 2Di). The micromolded ridges and grooves were about 15 and 3 µm wide respectively (Figure 2Dii). Thus, micromolding using a calcium loaded agar stamp facilitated precise control over surface topography of alginate thin films.

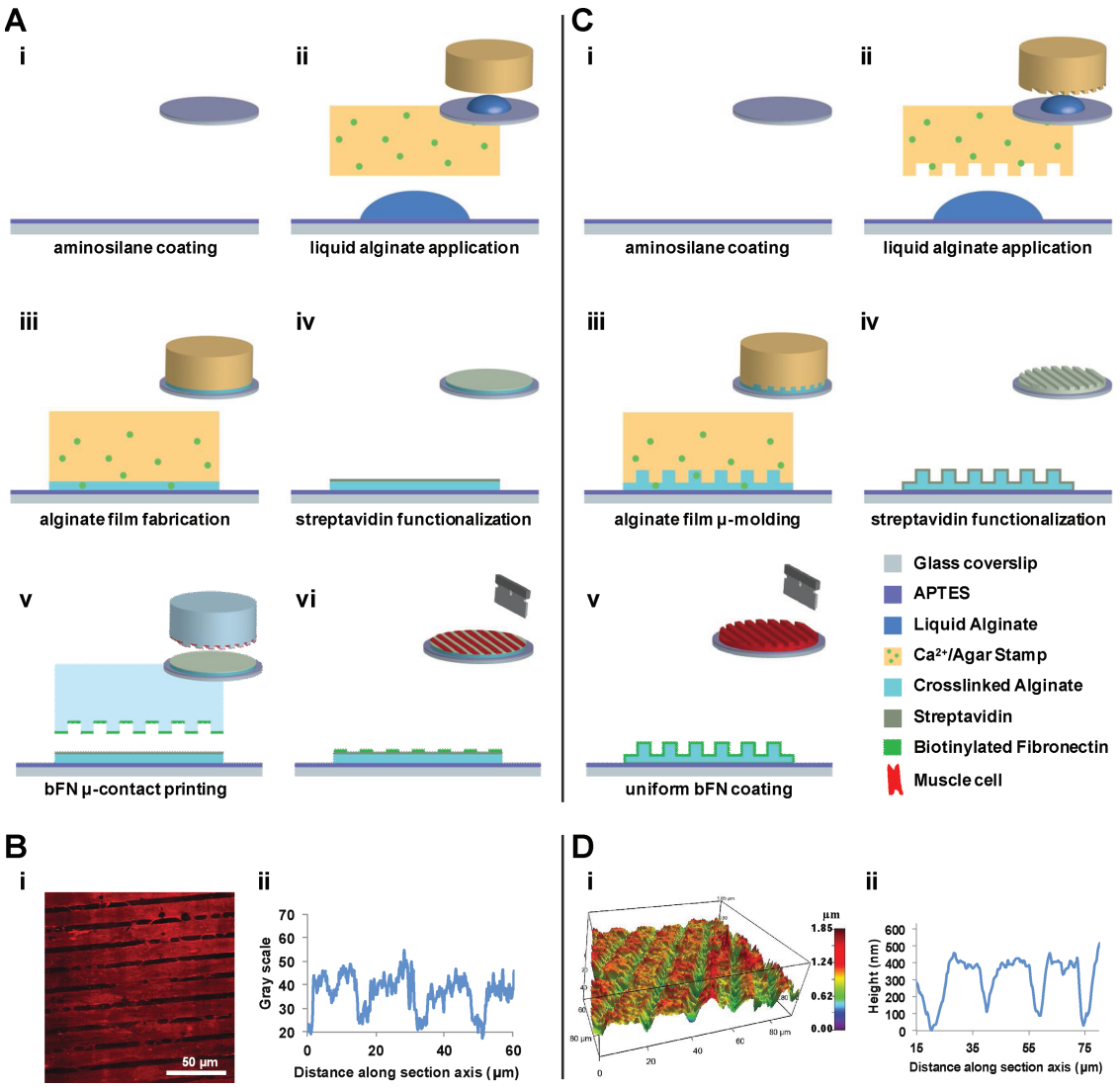

Figure 2. Micropatterned alginate thin films fabricated using A,B) microcontact printing and C,D) micromolding. A,Ci) A layer of APTES is deposited on the glass coverslip. A,Cii-iii) A flat or patterned calcium-loaded agar stamp is applied on a drop of alginate. A,C iv) The thin film of hydrogel is submerged in a solution of streptavidin mixed with the reagents EDC and sulfo-NHS and then washed and dried. A, Cv) Biotinylated fibronectin is applied either by microcontact printing with a stamp of PDMS or by simple submersion. A,Cvi) Samples are ready for being cut for contractility assay. Bi) Fluorescent imaging of immunostained 2D fibronectin pattern on flat alginate films. Bii) Section profile of fluorescence level. Di) 3D reconstruction of AFM imaging of the topography of micromolded films. Dii) Height profile along a section perpendicular to the features.

2.4. Cell Attachment and Tissue Alignment Onto Micropatterned Alginate thin Films

We asked if microcontact printed and micromolded alginate thin films could be used to engineer aligned cardiac and vascular smooth muscle tissue. After 72 h in culture, we observed that alginate surfaces coated uniformly with fibronectin through our biotin-streptavidin interactions could support a confluent isotropic monolayer of cardiac tissue (**Figure 3**Ai). We were also able to induce anisotropy in engineered cardiac tissue on micropatterned surfaces. Qualitative observations of the phase contrast images revealed that cells aligned and elongated along the pattern direction in both microcontact printed (Figure 3Bi) and micromolded samples (Figure 3Ci). Cardiac tissues were immunostained for nuclei, actin and sarcomeric α-actinin to visualize intracellular architecture. As is evident from the immunostains, cardiac myocytes seeded on microcontact printed alginate films (Figure 3Bii,iii and Figure 3Cii,iii) had global order and alignment as compared to cardiac myocytes on an isotropic coating of fibronectin (Figure 3Aii,iii). Similarly, flat alginate surfaces with a uniform coating of fibronectin could support an isotropic vascular smooth muscle layer (Figure 3D) while both microcontact printed (Figure 3E) and micromolded (Figure 3F) substrates resulted in anisotropy in engineered tissues. Thus, micropatterned alginate substrates could provide cues for cardiac and smooth muscle cells to form anisotropic tissue.

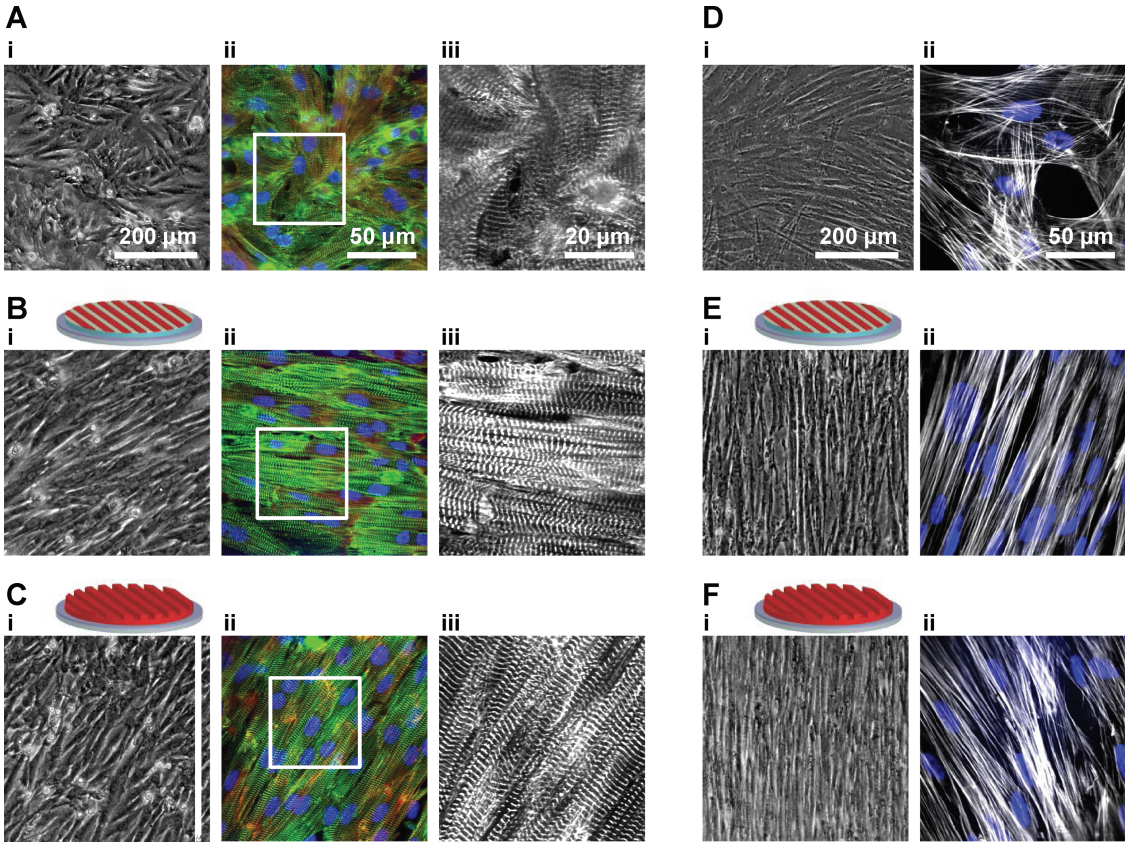

Figure 3. Tissues generated from A–C) cardiac myocytes and D–F) vascular smooth muscle cells on A,D) isotropic fibronectin, B,E) microcontact printed, and C,F) micromolded alginate substrates. A–Ci) Phase contrast pictures of cardiac tissues for each condition. A–Cii) Immunofluorescence composite images where actin is red, nuclei are blue and α-actinin is green and A–Ciii) zoomed-in grayscale images for α-actinin in white squares. D,Fi) Phase contrast pictures of vascular smooth muscle tissue for each condition and (D,Fii) Immunofluorescence composite images where actin is white and nuclei are blue.

Next, we sought to compare the anisotropy in intracellular architecture between the cultures on isotropic, microcontact printed and micromolded substrates. For cardiac cultures, quantification of sarcomere alignment was carried out using a modified fingerprint detection algorithm previously developed[6] to quantify sarcomeric Orientational Order Parameter (OOP).[8,33] OOP is extensively used in the analysis of spatial order in liquid crystals and ranges from a value of zero for completely random and isotropic sample to unity for perfectly aligned sample. Cardiac myocytes on the molded microgrooves and ridges (OOP = 0.48 ± 0.08, N = 6) were aligned as efficiently as on a microcontact printed surface (OOP = 0.46 ± 0.05, N = 6). Furthermore, alignment on both the surfaces was significantly better than on isotropic alginate surfaces (OOP = 0.31 ± 0.09). Sarcomeric OOP values are plotted in **Figure 4**A and are similar to the values previously reported for anisotropic monolayers engineered on PDMS substrates.[8] The anisotropy in vascular smooth muscle tissue was quantified by analyzing immunostains for F-actin. Actin OOP for both micromolded alginate (OOP = 0.94 ± 0.11, N = 6) and microcontact printed alginate (OOP = 0.98 ± 0.01, N = 6) was significantly more than on an isotropic alginate surface (OOP = 0.44 ±0.16, N = 6). Actin OOP values are plotted in Figure 4B and are similar to the reported values

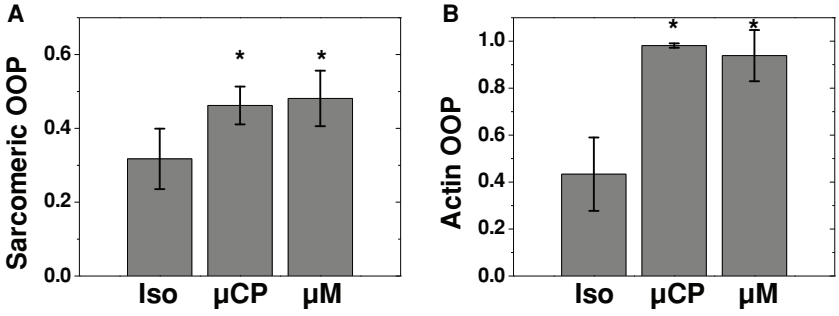

Figure 4. Orientational order parameter for A) sarcomeric alignment in cardiac tissue and B) F-actin alignment in vascular smooth muscle tissue cultured on isotropic alginate surface, microcontact printed alginate surface and micromolded alginate surface. (Mean ± SD, N = 6 coverslips with at least 3 fields of view of 160 µm × 160 µm per coverslip for each condition, * = statistically different from isotropic tissue, $p < 0.05$, OOP: Orientational Order Parameter, Iso: Isotropic fibronectin on flat alginate substrate, µCP: Microcontact printed lines of fibronectin on flat alginate, µM: Micromolded alginate substrate with a uniform coating of fibronectin).

for anisotropic vascular smooth muscle engineered on PDMS substrates.[10] Hence, the hydrogel micropatterning techniques described here were effective in creating anisotropic laminar monolayers of both striated and smooth muscle.

2.5. In Vitro Contractility Assay

We asked if two dimensional muscular tissues with controlled architecture on micropatterned alginate substrates could be adapted for functional contractility measurements. A muscular thin film (MTF) based contractility assay entails recording the three dimensional deformation of an elastic cantilever which is fixed to the substrate along one of the shorter edges, produced due to the two dimensional contraction of anisotropic muscular tissue engineered on top of it.[6–10] The deflection of the free edge is tracked and converted into tissue contractile stress under the assumption that the film acts as a two layer plane strain beam.[7,8]

Alginate films were precut into rectangular shapes prior to cell seeding (**Figure 5**Ai). Approximately 72 h after cell seeding, the cantilevers were peeled (Figure 5Aii) from the underlying glass substrate using sharp tweezers, and the deformation of the films was optically recorded under external electrical field stimulation (Figure 5Aiii). No sacrificial layer was needed in order to detach the cantilevers from the glass, and the thin films were stable enough to stay attached in the unpeeled regions (Figure 5B). In all the cases, the films contracted at the frequency of the external field stimulation, from 1 to 4 Hz. A representative example depicting the deformation of two films as observed by a stereoscope is shown in Figure 5C. In general, micropatterned alginate hydrogels could be successfully and repeatably utilized for building cardiac muscular thin film assays.

Next, we sought to quantify the stresses generated by alginate based cardiac MTFs. Figure 5D shows the stress profile of an alginate cardiac MTF under different stimulation regimes. The stress generated by the cardiac myocytes on this hybrid construct was directly measured using an automated tracking software.[7,8] Figure 5E,F show the stresses generated by cardiac tissue cultured on microcontact printed alginate and micromolded alginate substrates, respectively. These values are of the same order of magnitude as previously reported in anisotropic monolayers on stiff polydimethylsiloxane (of Young's modulus ~ 1000 kPa).[8] We should note that exact quantification of stresses could be complicated due to the following two factors: (i) Changes in mechanical properties of the alginate substrates over time and (ii) Presence of grooves and ridges in the micromolded alginate substrates contravening the two layer plane beam assumption made for calculating stresses. However, alginate gels made under similar conditions have been extensively characterized for their superior mechanical properties and utilized for long term tissue engineering applications.[25] Furthermore, the grooves in the micromolded substrates are less than 0.5 μm deep on the surface of typically 80 μm thick films. Hence the assumption of micromolded films are planar substrates for calculation of stresses should introduce minimal errors.

We asked whether micromolded alginate substrates could also reveal the slow and sustained contraction of vascular smooth muscle cells and support construction of VSM MTFs. Similar to cardiac experiments, alginate substrates were precut prior to cell seeding and 72 h after seeding, MTFs were peeled for recording contractile stresses. Immediately after peeling, VSM cantilevers assumed a baseline curvature (**Figure 6**A). At 10 min, MTFs were stimulated by a 100 nM dosage of a vasoconstrictor, endothelin-1. At 40 min, tissues were treated with a 100 μM dosage of a rho-kinase inhibitor, HA-1077 which made the tissues relax revealing their basal tone. Representative images of the endothelin-1 induced contraction and HA-1077 induced relaxation produced in 2 MTFs are shown in Figure 6B. Similar to cardiac MTFs, the edges of the cantilevers were optically tracked to quantify the stresses generated (Figure 6C). Contractile stress and basal tone are defined by the difference in the MTF tension prior to treatment (t = 0) and after the endothelin-1 exposure and HA-1077 exposure respectively.[10] The tension in the MTFs that remains even after the HA-1077 treatment is the passive residual stress. For tissues cultured on microcontact printed alginate substrates (Figure 6D), we measured average contraction stress, basal tone and residual stresses. In a similar manner, we made the same measurements for tissues on micromolded substrates (Figure 6E). Both the contraction stresses and basal tone generated by vascular smooth muscle tissues on alginate are at least an order of magnitude smaller than those reported previously on stiff PDMS substrates.[8,10] We observed high absolute values of residual stresses in the case of micromolded substrates which point to remodeling of the scaffold material by vascular smooth muscle tissue.

3. Discussion

Alginate hydrogels have been an active topic of research in the last decade for applications ranging from tissue regeneration[34] and drug delivery[35] to wound healing[36] and in vitro culture platforms.[37] Most of the applications take advantage of the fact that these hydrogels are mechanically and structurally similar to extracellular matrices and amenable to a variety of chemical modifications. Here, we utilize the carboxyl groups of the guluronic acids within alginate to react with the primary amines of the aminosilane coated glass coverslips as well as with the primary amines of streptavidin. This scheme enabled us to adhere alginate films to glass coverslips and covalently attach biotinylated fibronectin to alginate.

We tested the need for specific biotin-streptavidin interactions and found that if we omit the streptavidin inclusion with alginate and employed unmodified fibronectin, both cellular density and alignment was poor. To offset the relatively high cost of fibronectin, alginate hydrogels are often modified with cell-adhesive peptides. However, previous studies have highlighted the fact that even though cardiac myocytes adhered on peptide modified alginate surfaces,[22,38] the development of functional sarcomeric fibers did not occur as efficiently as on substrates coated with either fibronectin or laminin.[39] Hence, we chose to affix fibronectin onto micropatterned alginate surface for successful cell culture.

Our patterning techniques allowed creation of heterogeneities within the alginate soft matrix and both cardiac and

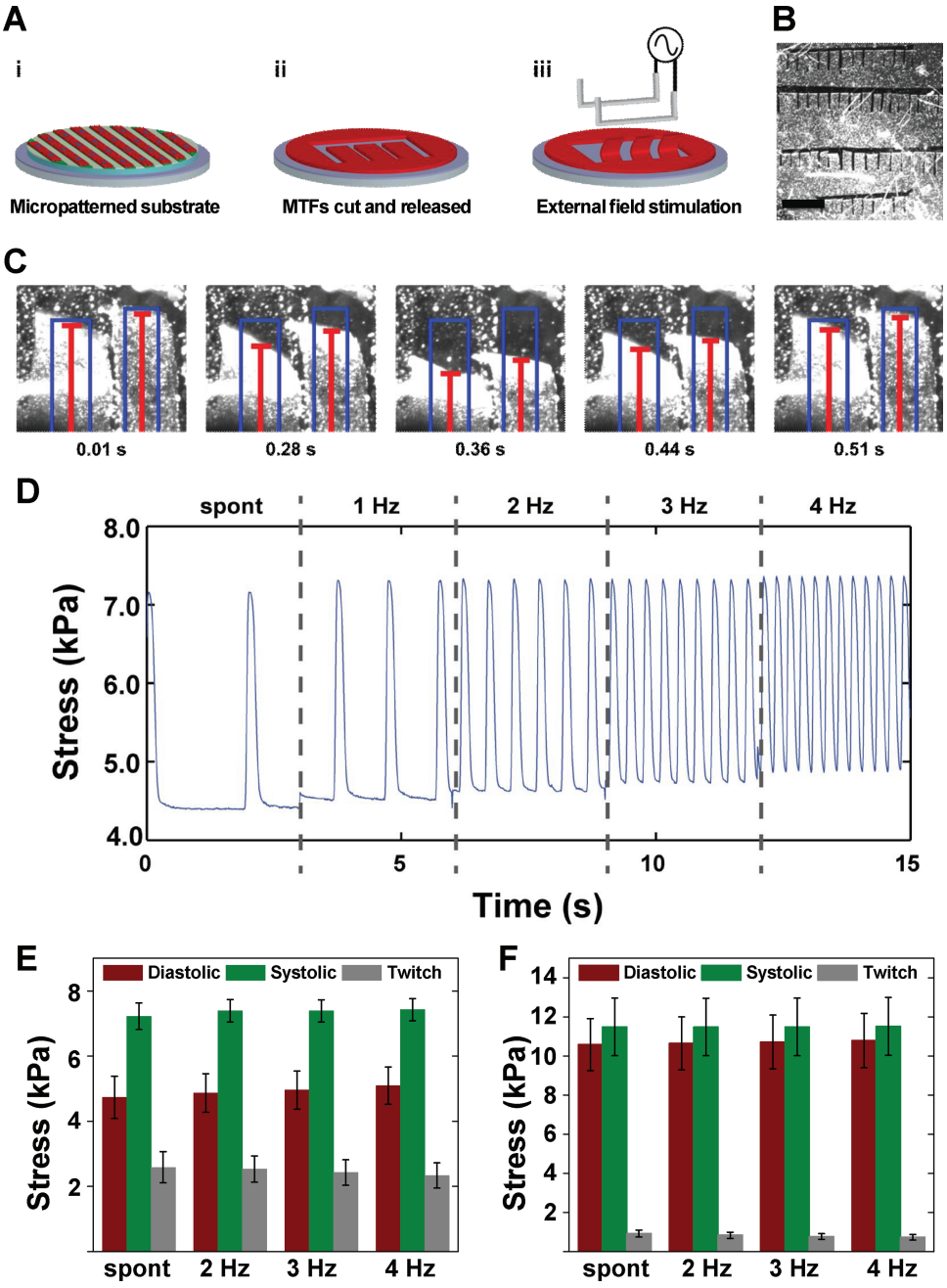

Figure 5. Results from cardiac muscular thin films constructed from micropatterned alginate substrates. A) Schematic of the assay: cantilevers are cut and peeled out of the alginate film and exposed to external electrical field stimulation. B) Optical photograph of the alginate coverslip after peeling the cut regions showing a high number of MTFs from a single experiment. Scale bar represents 5 mm. C) Tracking of the horizontal projection of the 2 representative films during one contraction cycle at 2 Hz stimulation frequency. D) Representative time trace of stress generated by one MTF at different pacing frequencies. Average diastolic, peak systolic and twitch stresses generated by E) microcontact printed and F) micromolded alginate cardiac MTFs. (Mean ± SEM, N = 7 MTFs in (E) and N = 6 MTFs in (F), spont = spontaneous contraction).

vascular smooth muscle cells could attach and align anisotropically along those boundary conditions leading to anisotropic muscular tissues. The resulting tissue deformed the alginate substrate synchronously, pacing at the frequency of field stimulation in the case of cardiac tissue and responding to vasoconstrictors and vasodilators in the case of smooth muscle tissue. We were also able to quantify muscular tissue-level stresses in vitro. Previous studies have shown that the stress generated by cardiac tissues is in the order of magnitude of a few kPa both in vitro[8] for engineered neonatal rat cardiac muscle and ex vivo[40] for adult rat right ventricular papillary muscles. Thus, our data suggests that an engineered cardiac tissue on alginate thin films generates contractile stresses comparable to that reported for healthy myocardium. While cardiac tissue did not

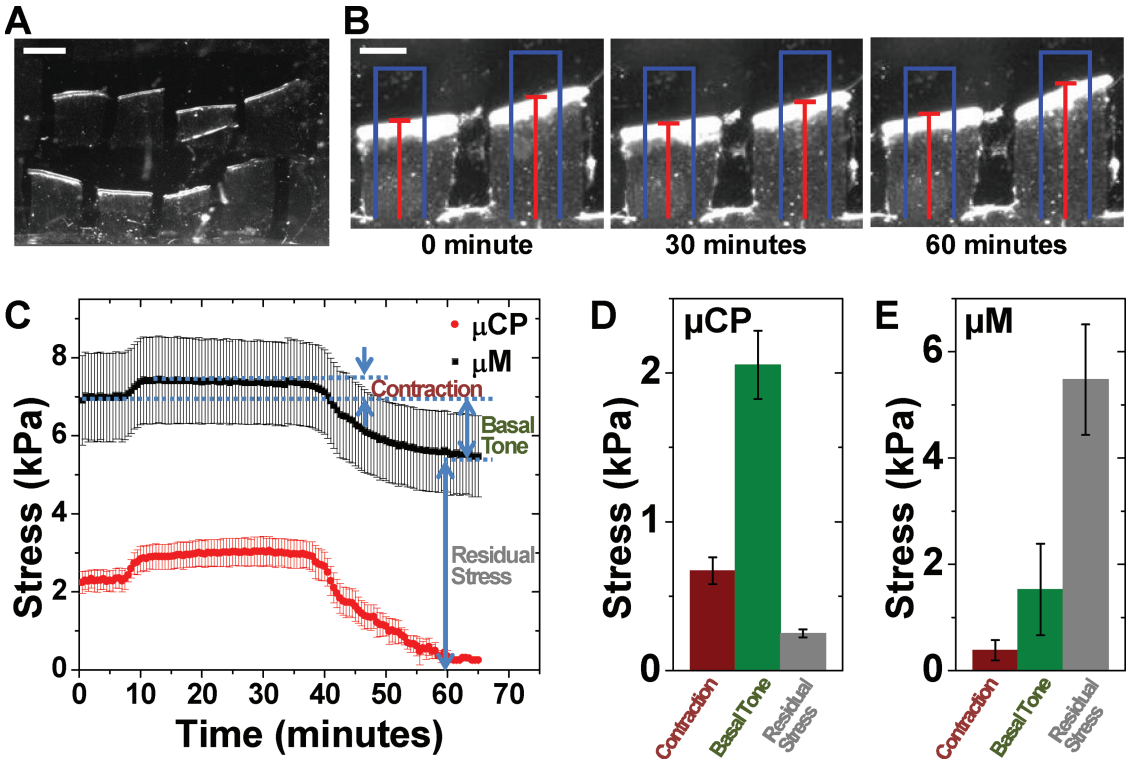

Figure 6. Results from vascular smooth muscle thin films constructed from micropatterned alginate substrates. A) Optical photograph of the alginate coverslip after peeling the cut regions and peeling the MTFs. Scale bar represents 1 mm. B) Tracking of the horizontal projection of the 2 representative films during one experiment; no treatment at 0 min, after stimulation with endothelin-1 at 30 min and after exposure to HA-1077 at 60 min. Scale bar represents 1 mm. C) Averaged time traces of stress generated by engineered vascular smooth muscle on microcontact printed (red circles, N = 7) and micromolded (black squares, N = 21) alginate MTFs. Untreated samples are stimulated by 100 nM endothelin-1 at 10 min and treated with 100 μM HA-1077 at 40 min. The calculation of contraction stress generated in response to vasoconstrictor treatment, basal tone revealed by vasodilator treatment and the residual stress are indicated in the panel. Average contraction stress, basal tone and residual stresses recorded on D) microcontact printed and E) micromolded alginate vascular smooth muscle MTFs (Mean ± SEM, N = 7 MTFs in (D) and N = 21 MTFs in (E)).

exhibit residual passive stress, vascular tissue on micromolded substrates did. We suspect that this may be due to the sustained smooth muscle contraction and its effects on the 3D surface topology of the micromolded substrate.

Interestingly, alginate substrates micropatterned with cell adhesion proteins like fibronectin also provide many advantages that are required for a successful cardiac patch. Recent advances have made possible the incorporation and release of chemical agents such as VEGF[23] or anti-apoptotic factors[41] from within the alginate. We believe that cellular remodeling of the micromolded alginate substrate could be advantageous, facilitating the release of medicinal therapeutics embedded in the alginate scaffold. It is envisioned that an anisotropic tissue pattern, which is sustainable over a long time, could all lead to an optimal integration of the patch inside the heart, with reduction of the ischemic area by progressive revascularization of the structure.

In summary, we recapitulate the anisotropic alignment of muscular tissue on ECM stiffness mimicking substrates and achieve physiologically relevant contractile stress levels. MTF fabrication procedure is simplified by the fact that we do not need a sacrificial layer to release the alginate MTFs from the glass coverslip leading to a higher throughput "muscle-on-a-chip". For in vitro drug development studies, the micromolding of substrates enables a straightforward route to incorporation of the MTFs inside a microfluidic device which is critical for connection to other in vitro organ mimics upstream or downstream. Indeed, one of the major challenges of incorporating a patterned surface in a microfluidic device is the need to plasma-treat the two sides of the chamber. This can deleteriously affect the bioactivity of any extracellular matrix protein micropatterned on the substrate. A micromolded system allows for uniform coating of the films after sealing of the device. It is important to note that the 3D patterns created by the micromolding technique needed considerably more optimization efforts as they were more susceptible to deterioration due to user perturbations. On the other hand, microcontact printing of fibronectin on soft alginate substrates opens up the opportunity to conduct classical traction force microscopy experiments. Inclusion of fiduciary fluorescent particles within the alginate would open opportunities for detailed cardiac biophysics and physiology studies.

4. Conclusions

Here, we reported two successful techniques for micropatterning soft alginate substrates: i) microcontact printing of

cell-adhesive proteins and ii) micromolding followed by a uniform coating of proteins. The heterogeneity in fibronectin pattern in microcontact printed substrates and heterogeneity in topography in micromolded substrates lead to formation of anisotropic cardiac and vascular smooth muscle tissues. We also demonstrate the potential of resulting alginate muscular thin films for in vitro assays for muscular contractility. These patterned films could be employed in the next generation contractility assays as well as various tissue engineering applications thanks to their flexibility in terms of stiffness, chemical and physical patterns, and a broad variety of extracellular matrix proteins that can be incorporated at the surface of the film through streptavidin-biotin coupling.

5. Experimental Section

Fabrication of Alginate Thin Films: Calcium-loaded agar stamps were prepared as previously reported.[24] Briefly, an aqueous solution of 5% Agar (Sigma-Aldrich, St. Louis, MO) was melted and mixed with $CaCl_2$ dihydrate (Sigma-Aldrich, St. Louis, MO) of different concentrations. The concentrations were chosen to allow for rapid gel formation without affecting the mechanical properties of the resulting hydrogel. The mixture of agar and $CaCl_2$ was then poured on silicon wafers with different patterns made by traditional photolithographic methods. The agar was left for 30 min at room temperature and then stamps were punched out of the main slab and stored at 4 °C until use.

Aminosilane coated glass coverslips were prepared to enhance the adhesion of the alginate thin films. 18 mm diameter coverslips were washed with ethanol and dried with nitrogen. They were then placed in a UV-Ozone generator (Jelight Company, Inc., Irvine, CA) for 8 min to activate the glass. They were placed for 30 min in a solution made of 5% aminopropyltriethoxysilane (APTES), 5% Milli-Q water and 90% pure ethanol. The coverslips were then washed in 100% ethanol and in Milli-Q water and stored for 30 min at 65 °C.

To fabricate the films of alginate, a 40 µL drop of 5% w/v alginate (Alginic acid, sodium salt from brown algae, A2158, Sigma-Aldrich, St. Louis, MO) was poured on top of the previously made aminosilane coated coverslips. Alginate solution was supplemented with 5 mg/mL Sulfo-NHS (Pierce, Rockford, IL) and 10 mg/mL EDC (Pierce, Rockford, IL) to allow the carboxylic groups of the guluronic acids to react with the primary amines of the APTES coated coverslips. Immediately after, the agar stamp, either flat or patterned, was applied on the drop and left for ~20 s to complete the crosslinking. After removal of the stamp, the coverslips were shortly washed in Milli-Q water and then placed in a solution of 1% $CaCl_2$, in order to maintain equilibrium of calcium concentration. The buffer was then replaced by a solution of 5 mg/mL Sulfo-NHS (Pierce, Rockford, IL) and 10mg/mL EDC (Pierce, Rockford, IL) and 50 µg/mL of streptavidin (Invitrogen, Carlsbad, CA) and the coverslips were left on a horizontal shaker for 4 h at room temperature. The coverslips were then washed with a solution of 1% $CaCl_2$ and left under laminar flow for drying. Once dried, they were either incubated with a solution of 50 µg/mL biotinylated fibronectin (micromolded films) or they were microcontact printed using a PDMS (Sylgard 184, Dow Corning, Midland, MI) stamp incubated with 25µg/mL biotinylated fibronectin and dried. In both cases, the biotinylated fibronectin was applied for 15 min. The coverslips were left under laminar flow again to be dry enough to be cut. Shapes of cantilevers were cut inside the films and the coverslips were placed back in 1% $CaCl_2$ until cell seeding.

Stiffness Measurement: The Young's modulus in compression was derived from stress-strain curves obtained using an Instron 3342 mechanical apparatus (Instron, Norwick, MA) in uniaxial unconfined compression mode. Briefly, alginate pieces were crosslinked in calcium-loaded agar gels previously punched to form 8mm-diameter holes. After the alginate had been fully crosslinked, the height of the cylinder of alginate were measured and placed in the apparatus and the strain was recorded at different loads. The Young's modulus in compression was calculated as the slope at the beginning of the deformation, where the curve can be assumed to be linear.

Thickness Measurement: Fluorescein isothiocyanate (FITC) was added to the solution of 5% w/v alginate at a ratio of 1:100 to alginate. Coverslips were then placed in a circular coverslip holder and imaged through laser scanning confocal microscope. Stacks were acquired every 0.46 µm and the average fluorescence was plotted for every stack in order to detect where the fluorescence started and ended.

Atomic Force Microscopy: 3D topographical scans of the micromolded alginate thin films were recorded using contact mode atomic force microscopy (AFM) on a MFP-3D-IO AFM (Asylum Research, Santa Barbara, CA) mounted on a Zeiss Axiovert 200 MAT. Aluminum coated silicon probes with spring constants of 0.1 N/m (Vista Probes, Phoenix, AZ) were used during AFM.

Biotinylated Fibronectin Preparation: Human fibronectin (BD Biosciences, Bedford, MA) was resuspended in filter sterilized low resistance Milli-Q water at a concentration of 1 mg/mL. EZ-Link Sulfo-NHS-LC-Biotin and dialysis cassettes were purchased from Thermo Fischer Scientific Inc., Rockford, IL. The reaction between the biotin and the fibronectin was performed according to the manufacturer's instructions. The product of the reaction was then dialyzed against PBS and the PBS was replaced every hour. Then, the solution was diluted at an approximate concentration of 1 mg/mL in PBS and stored at 4 °C until use.

Cardiac Myocyte Harvest, Seeding, and Culture: All procedures were conducted according to the guidelines of the Harvard University Animal Care and Use Committee. Cardiac myocytes were extracted from neonatal rat ventricles using previously described protocols.[8,42] As a result of the harvest and cardiac myocyte enrichment, the cell mixture contains also a very small quantity of cardiac fibroblasts. Samples were cultured in 12-well plates at a cell density of 400 000/cm^2 in Medium 199 supplemented with 10% heat-inactivated fetal bovine serum (FBS, Invitrogen, Carlsbad, CA), 10 mM HEPES, 0.1 mM MEM non-essential amino acids, 20 mM glucose, 2 mM L-glutamine, 1.5 µM vitamin B-12, and 50 U/mL penicillin for 1 day. After attachment of the cells on the alginate films, cells were washed with PBS and incubated in fresh culture medium with 10% FBS. On day 2, the serum concentration was reduced to 2% in order to reduce fibroblast proliferation.

Vascular Smooth Muscle Cell Seeding and Culture: Human umbilical artery vascular smooth muscle cells (Lonza, Walkersville, MD) were cultured in growth medium consisting of M199 culture medium (GIBCO, Invitrogen, Carlsbad, CA) supplemented with 10% fetal bovine serum (Invitrogen), 10 mM HEPES, 20 mM glucose, 2 mg/mL vitamin B-12, 50 U/mL penicillin and 50´U/mL streptomycin. All experiments were performed at passage 4–7. Cells were seeded at 10 000/cm^2 in the same growth media and incubated till they reached confluence.

Contractility Assay and Electrical Field Stimulation: The contractility assay was performed under a stereoscope coupled to a National Instruments LabVIEW board to allow controlled live recording of thin film contraction. Samples were placed in a 35-mm-diameter petri dish filled with a Tyrode's solution (137 mM NaCl, 5.4 mM KCl, 1.2 mM $MgCl_2$, 1 mM $CaCl_2$, 20 mM HEPES, pH = 7.4). A lid with two electrodes connected to a field stimulator (Myopacer, IonOptix Corp., Milton, MA) was placed on top of the dish, making sure that the electrodes were dipping in the solution for field stimulation. The dish was placed in a heating plate to control that the experiment was performed at 37 °C. After peeling the precut cantilevers, spontaneous contraction of the films was recorded. Then, field stimulation was performed at different frequencies (stimulation frequency from 1 to 4 Hz, external voltage from 5 to 15 V with a square pulse of duration 10 ms), and the sample was filmed throughout the experiment, at a frame rate of 120 fps.

Contractility Analysis: The cantilever radius of curvature was derived using a MATLAB code and analyzing videos cleaned with ImageJ to reduce the background noise. Knowing the stiffness and thickness of the hybrid construct, the stress generated by the cantilever under field stimulation was calculated using a previously published model.[7] Stresses were calculated using the methods developed for PDMS MTFs for cardiac[8] and vascular smooth muscle tissues.[9]

Immunostaining and Structure Characterization: After contractility assay, the samples were washed in warm PBS (at 37 °C) supplemented with 0.02% $CaCl_2$. Then, they were incubated for 15 min in a warm solution of 4% Paraformaldehyde (PFA) and 0.5 µL/mL of TritonX-100 in PBS. Cardiac samples were then washed with PBS and placed upside down on 200 µL of a solution of PBS containing 1 µL DAPI, 1 µLAlexa Fluor633-conjugated Phalloidin (A22284, Invitrogen, Carlsbad, CA), 1 µL polyclonal anti-human fibronectin antibody (F3648, Sigma-Aldrich, St. Louis, MO), and 1 µL monoclonal anti-sarcomeric α-actinin (A7732 clone EA-53, Sigma-Aldrich, St. Louis, MO) for 1 h at room temperature. Samples were then washed in PBS and incubated for 1 h with the corresponding Alexa Fluor-488 and -546 fluorescently labeled secondary antibodies. For fibronectin, a goat anti rabbit Alexa Fluor-546 antibody was used (A-11035, Invitrogen, Carlsbad, CA). For α-actinin, a goat anti-mouse Alexa Fluor-488 antibody was used (A-11001, Invitrogen, Carlsbad, CA). The vascular smooth muscle samples were exposed to 200 µL of a solution of PBS containing 1 µL DAPI, 1 µL Alexa Fluor633-conjugated Phalloidin (A22284, Invitrogen, Carlsbad, CA), 1 µL polyclonal anti-human fibronectin antibody (F3648, Sigma-Aldrich, St. Louis, MO) for the primary staining and to corresponding goat anti rabbit Alexa Fluor-546 antibody (A-11035, Invitrogen, Carlsbad, CA) for secondary staining of fibronectin. The samples were then washed with PBS and mounted on microscope glass slides before fluorescent imaging on a Zeiss LSM 7 LIVE confocal microscope. Fluorescent immunostains of α-actinin in the cardiac samples and immunostains of actin in the vascular smooth muscle samples were processed using a MATLAB code based on fingerprint detection as previously reported.[5–8] After extraction of the main pattern, the angle distribution was analyzed and orientational order parameter reported.

Acknowledgements

A.A. and Y.F. contributed equally to this work. The authors acknowledge the support from Harvard Materials Research Science and Engineering Center under NSF award number DMR-0213805, NIH/NINDS grant 1 U01 NS073474-01, and the Harvard Center for Nanoscale Systems for the use of clean room facilities.

Received: November 12, 2012
Revised: December 22, 2012
Published online: March 19, 2013

[1] H. T. H. Au, B. Cui, Z. E. Chu, T. Veres, M. Radisic, *Lab Chip* **2009**, *9*, 564.
[2] M. P. Prabhakaran, J. Venugopal, D. Kai, S. Ramakrishna, *Mater. Sci. Eng., C* **2011**, *31*, 503.
[3] D. H. Kim, E. A. Lipke, P. Kim, R. Cheong, S. Thompson, M. Delannoy, K. Y. Suh, L. Tung, A. Levchenko, *Proc. Natl. Acad. Sci. USA* **2010**, *107*, 565.
[4] X. H. Zong, H. Bien, C. Y. Chung, L. H. Yin, D. F. Fang, B. S. Hsiao, B. Chu, E. Entcheva, *Biomaterials* **2005**, *26*, 5330.
[5] M. R. Badrossamay, H. A. McIlwee, J. A. Goss, K. K. Parker, *Nano Lett.* **2010**, *10*, 2257.
[6] A. W. Feinberg, A. Feigel, S. S. Shevkoplyas, S. Sheehy, G. M. Whitesides, K. K. Parker, *Science* **2007**, *317*, 1366.
[7] P. W. Alford, A. W. Feinberg, S. P. Sheehy, K. K. Parker, *Biomaterials* **2010**, *31*, 3613.
[8] A. Grosberg, P. W. Alford, M. L. McCain, K. K. Parker, *Lab Chip* **2011**, *11*, 4165.
[9] A. Grosberg, A. P. Nesmith, J. A. Goss, M. D. Brigham, M. L. McCain, K. K. Parker, *J. Pharmacol. Toxicol. Methods* **2012**, *65*, 126.
[10] P. W. Alford, A. P. Nesmith, J. N. Seywerd, A. Grosberg, K. K. Parker, *Integr. Biol.* **2011**, *3*, 1063.
[11] A. J. Engler, M. A. Griffin, S. Sen, C. G. Bonnetnann, H. L. Sweeney, D. E. Discher, *J. Cell Biol.* **2004**, *166*, 877.
[12] A. J. Engler, C. Carag-Krieger, C. P. Johnson, M. Raab, H. Y. Tang, D. W. Speicher, J. W. Sanger, J. M. Sanger, D. E. Discher, *J. Cell Sci.* **2008**, *121*, 3794.
[13] A. J. Engler, S. Sen, H. L. Sweeney, D. E. Discher, *Cell* **2006**, *126*, 677.
[14] N. Huebsch, P. R. Arany, A. S. Mao, D. Shvartsman, O. A. Ali, S. A. Bencherif, J. Rivera-Feliciano, D. J. Mooney, *Nat. Mater.* **2010**, *9*, 518.
[15] D. Kai, M. P. Prabhakaran, G. R. Jin, S. Ramakrishna, *J. Biomed. Mater. Res. Part B* **2011**, *98B*, 379.
[16] G. C. Engelmayr, M. Y. Cheng, C. J. Bettinger, J. T. Borenstein, R. Langer, L. E. Freed, *Nat. Mater.* **2008**, *7*, 1003.
[17] A. D. Augst, H. J. Kong, D. J. Mooney, *Macromol. Biosci.* **2006**, *6*, 623.
[18] K. Y. Lee, D. J. Mooney, *Prog. Polym. Sci.* **2012**, *37*, 106.
[19] O. Tsur-Gang, E. Ruvinov, N. Landa, R. Holbova, M. S. Feinberg, J. Leor, S. Cohen, *Biomaterials* **2009**, *30*, 189.
[20] J. Yu, Y. Gu, K. T. Du, S. Mihardja, R. E. Sievers, R. J. Lee, *Biomaterials* **2009**, *30*, 751.
[21] J. S. Yu, K. T. Du, Q. Z. Fang, Y. P. Gu, S. S. Mihardja, R. E. Sievers, J. C. Wu, R. J. Lee, *Biomaterials* **2010**, *31*, 7012.
[22] Y. Sapir, O. Kryukov, S. Cohen, *Biomaterials* **2011**, *32*, 1838.
[23] X. Hao, E. A. Silva, A. Mansson-Broberg, K.-H. Grinnemo, A. J. Siddiqui, G. Dellgren, E. Wardell, L. A. Brodin, D. J. Mooney, C. Sylven, *Cardiovasc. Res.* **2007**, *75*, 178.
[24] G. T. Franzesi, B. Ni, Y. B. Ling, A. Khademhosseini, *J. Am. Chem. Soc.* **2006**, *128*, 15064.
[25] M. M. Stevens, H. F. Qanadilo, R. Langer, V. P. Shastri, *Biomaterials* **2004**, *25*, 887.
[26] M. F. Berry, A. J. Engler, Y. J. Woo, T. J. Pirolli, L. T. Bish, V. Jayasankar, K. J. Morine, T. J. Gardner, D. E. Discher, H. L. Sweeney, *Am. J. Physiol.: Heart Circ. Physiol.* **2006**, *290*, H2196.
[27] S. Zhang, A. Sun, H. Ma, K. Yao, N. Zhou, L. Shen, C. Zhang, Y. Zou, J. Ge, *J. Cell. Mol. Med.* **2011**, *15*, 2245.
[28] H. Abe, K. Hayashi, M. Sato, *Data book on mechanical properties of living cells, tissues, and organs*, Springer-Verlag, New York **1996**.
[29] R. J. Pelham, Y. L. Wang, *Proc. Natl. Acad. Sci. USA* **1997**, *94*, 13661.
[30] A. Mata, A. J. Fleischman, S. Roy, *Biomed. Microdevices* **2005**, *7*, 281.
[31] J. Yeh, Y. Ling, J. M. Karp, J. Gantz, A. Chandawarkar, G. Eng, J. Blumling III, R. Langer, A. Khademhosseini, *Biomaterials* **2006**, *27*, 5391.
[32] A. Khademhosseini, G. Eng, J. Yeh, J. Fukuda, J. Blumling III, R. Langer, J. A. Burdick, *J. Biomed. Mater. Res., Part A* **2006**, *79A*, 522.
[33] A. Grosberg, P.-L. Kuo, C.-L. Guo, N. A. Geisse, M.-A. Bray, W. J. Adams, S. P. Sheehy, K. K. Parker, *PLoS Comput. Biol.* **2011**, *7*.
[34] E. G. Popa, M. E. Gomes, R. L. Reis, *Biomacromolecules* **2011**, *12*, 3952.
[35] H. H. Tonnesen, J. Karlsen, *Drug Dev. Ind. Pharm.* **2002**, *28*, 621.
[36] V. M. Donaghue, J. S. Chrzan, B. I. Rosenblum, J. M. Giurini, G. M. Habershaw, A. Veves, *Adv. Wound Care* **1998**, *11*, 114.
[37] S.-F. Lan, B. Starly, *Toxicol. Appl. Pharmacol.* **2011**, *256*, 62.
[38] F. Rask, S. M. Dallabrida, N. S. Ismail, Z. Amoozgar, Y. Yeo, M. A. Rupnick, M. Radisic, *J. Biomed. Mater. Res., Part A* **2010**, *95A*, 105.
[39] S. Y. Boateng, S. S. Lateef, W. Mosley, T. J. Hartman, L. Hanley, B. Russell, *Am. J. Physiol.: Cell Physiol.* **2005**, *288*, C30.
[40] M. B. Effron, G. M. Bhatnagar, H. A. Spurgeon, G. Ruanoarroyo, E. G. Lakatta, *Circ. Res.* **1987**, *60*, 238.
[41] L. L. Y. Chiu, M. Radisic, G. Vunjak-Novakovic, *Macromol. Biosci.* **2010**, *10*, 1286.
[42] W. J. Adams, T. Pong, N. A. Geisse, S. Sheehy, K. K. Parker, *J. Comput. Aided Mater. Des.* **2007**, *14*, 19.